

Nonequilibrium solidification of poly(ethylene oxide)–sodium thiocyanate mixtures

B. CRIST, Y. L. LEE

Department of Materials Science and Engineering, Northwestern University, Evanston, Illinois 60208, USA

Mixtures of polyethylene oxide (PEO) and sodium thiocyanate (NaSCN) were isothermally crystallized at temperatures between 7 and 37°C, below the eutectic temperature $T_e = 63^\circ\text{C}$. The stable phases are semicrystalline polyethylene oxide, SPEO, and a crystalline complex, CC, with the formula PEO_3NaSCN ; these two solids grow by different mechanisms. Salt mole fraction was varied between $0.067 \leq X \leq 0.143$ for studies by optical microscopy and differential scanning calorimetry. Solidification was observed to proceed by primary growth followed by coupled growth at a nonequilibrium composition X'_e much greater than the equilibrium eutectic composition $X_e = 0.026$. The boundaries of this skewed coupled zone could not be determined because of a dependence of X'_e on the nature of the primary phase.

1. Introduction

Mixtures of polar polymers and salts have been the subject of considerable interest, primarily because of the ionic conductivity of such systems [1, 2]. Poly(ethylene oxide), PEO, is the polymer employed most frequently as the “host” or solvent for various salts which typically have alkali metal cations. PEO is itself a crystallizable polymer, and also forms crystalline complexes of the type PEO_nMA , where M represents the cation and A the anion of the salt. In addition to crystalline PEO and the crystalline complex (hereafter abbreviated CC), noncrystalline regions composed of salt dissolved in amorphous PEO are usually present. Ionic conductivity has been shown to result almost exclusively from mobile ions in these amorphous regions [1–4]. At higher temperatures the amorphous phase is a liquid in equilibrium with CC, while at temperatures below the normal melting temperature of PEO, $T_m = 65^\circ\text{C}$, conduction occurs through the amorphous component of semicrystalline PEO; here the salt is dissolved in noncrystalline regions between lamellar PEO crystals.

The relations between overall composition, temperature and phases in such systems can be expressed by binary phase diagrams as first done by Sorensen and Jacobsen [5] for $\text{PEO-LiCF}_3\text{SO}_3$. Figure 1 is for melt-equilibrated PEO-NaSCN [4] in which the terminal phases are CC and semicrystalline PEO, abbreviated SPEO. The composition is expressed as mole fraction of salt based on monomer repeats in PEO, i.e.

$$X = \frac{\text{NaSCN}}{\text{NaSCN} + -\text{CH}_2\text{CH}_2\text{O}-}$$

where the chemical formulas represent the number of moles of each component. This phase diagram is typical of many PEO–salt systems, having a eutectic

point at a SPEO-rich composition ($X_e = 0.026$) and a CC phase of composition X_{cc} which is independent of temperature. It differs from other treatments [5–9], however, in that the salt is accorded a finite solubility in SPEO. This feature is essential for characterizing the concentration and temperature dependence of ionic conductivity at temperatures below the eutectic temperature $T_e = 63^\circ\text{C}$ [4].

Presented here is a study of the solidification of PEO-NaSCN from the melt. The two terminal phases, SPEO and CC, precipitate from the liquid by different mechanisms and generally at very different rates. SPEO forms conventional spherulites (Fig. 2a) which grow at a constant rate determined by molecular nucleation at the crystal–melt interface [10]. The growth of the polycrystalline CC aggregates (see Fig. 2b), on the other hand, is determined by the diffusion rate of salt to the growth front [11]. Growth rate in the two-phase $L + \text{CC}$ phase field above T_e is small, with tens or hundreds of hours required to establish equilibrium. Thus hypereutectic liquids of PEO and NaSCN are easily quenched below the eutectic temperature $T_e = 63^\circ\text{C}$. Some aspects of melt crystallization of similar PEO-NaSCN systems have been given in a recent report by Robitaille *et al.* [9]. It is shown here that the two-phase morphology evolves from undercooled liquids by growth of a primary phase followed by a eutectic reaction at a composition near that determined by the extension of the liquidus line of the fastest growing (SPEO) component. This behaviour is consistent with established principles of non-equilibrium solidification in binary eutectic systems [12, 13].

2. Experimental procedure

Solutions of PEO (Polyscience, nominal $M = 600\,000$) in acetone (Mallinkrodt, reagent grade) and NaSCN

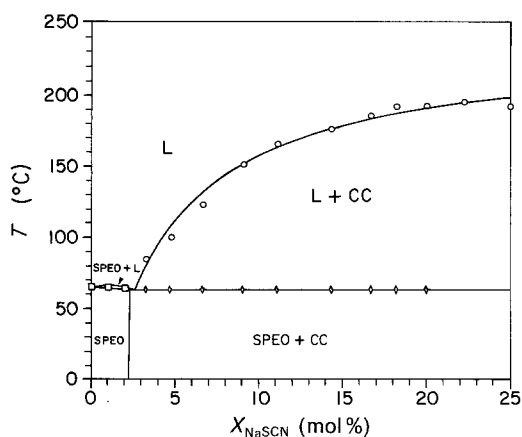


Figure 1 Partial phase diagram of PEO–NaSCN, with terminal phases SPEO and the complex crystalline compound PEO_3NaSCN .

(Aldrich, reagent grade) in methanol (American Scientific Products, anhydrous AR) were prepared and blended at room temperature to achieve the desired stoichiometry. Films were cast by evaporating the solvent in air for 24 h and in vacuum (10^{-3} torr) at room temperature for a further 24 h. These dried solution cast films were then heated to 130°C and cooled over a 30 min period to room temperature. No special precautions were taken to prevent contact with water vapour, though samples were stored in a desiccator when not in use.

Optical microscopy was performed with a Leitz Ortholux transmission microscope with crossed polarizer and analyser. The microscope was equipped with a Mettler FP5 hot stage and a 35 mm camera. Samples were thin ($\sim 50\ \mu\text{m}$) films between glass slides. In these experiments and in the DSC work below, melting temperatures and salt concentrations were chosen to avoid the precipitation of pure NaSCN from the mixtures.

A Perkin-Elmer DSC-2 was used for differential scanning calorimetry. The DSC samples ($\sim 10\ \text{mg}$) were melted, then cooled at the maximum rate (nominally $320\ \text{K}\ \text{min}^{-1}$) to $160\ \text{K}$ (-113°C), quenching them to a glassy state. The temperature was then slewed to the crystallization temperature T_c for the desired time t_c , after which the temperature was decreased once again to $160\ \text{K}$, arresting the crystalliz-

ation process. The partially crystallized sample was then analysed by the final DSC scan at $20\ \text{K}\ \text{min}^{-1}$, with sensitivity adjusted to observe the heat capacity step indicating T_g of the amorphous PEO–NaSCN. T_g is taken as the midpoint of the heat capacity step.

3. Results and discussion

3.1. Phase diagram

The phase diagram in Fig. 1 is the same as that published earlier [4], though the stoichiometry of the CC phase, $X_{cc} = 0.25$, is adjusted to conform to PEO_3NaSCN . This agrees with the results of Robitaille *et al.* [9]. The stoichiometry determined previously in these laboratories was based on DSC analysis of samples cooled from 130°C to room temperature in about 30 min. Reanalysis of samples having $X = 0.22$ prepared by slow-cooling from 185°C ($< 0.5^\circ\ \text{min}^{-1}$) or solution casting show a small endotherm corresponding to the eutectic melting of SPEO; those with $X = 0.25$ have no such melting peak. Hence the composition of properly equilibrated CC is very close to $X_{cc} = 0.25$. This small change does not influence significantly the calculated temperature or concentration dependence of conductivity based on ions dissolved in amorphous portion of the complex.

The eutectic point in Fig. 1 ($X_e = 0.026$, $T_e = 63^\circ\text{C}$) differs slightly from that reported recently by Robitaille *et al.* ($X_e = 0.039$, $T_e = 54^\circ\text{C}$) for melt crystallized PEO–NaSCN in which the polymer had molecular weight $M = 4000$ [9]. Uncertainties in extrapolating the liquidus line to T_e presumably cause the discrepancy in X_e . The difference in eutectic temperatures arises mainly from the dependence of melting temperature T_m on the molecular weight of PEO [14]. Additionally, there is the question of crystallinity of the terminal PEO (or SPEO) phase. The heat of fusion of PEO used here ($M = 600\ 000$, melt crystallized) is $150\ \text{J}\ \text{g}^{-1}$ whereas that observed by Robitaille *et al.* is $192\ \text{J}\ \text{g}^{-1}$ [9]. These correspond to crystallinities of 0.76 and 0.97, respectively, using $197\ \text{J}\ \text{g}^{-1}$ as the heat of fusion of perfect crystalline PEO [14]. This difference is once again largely attributable to the disparate molecular weights of the two polymers employed; high M polymers have crystallinities limited by kinetic factors, especially when solidified from the melt. Since any salt

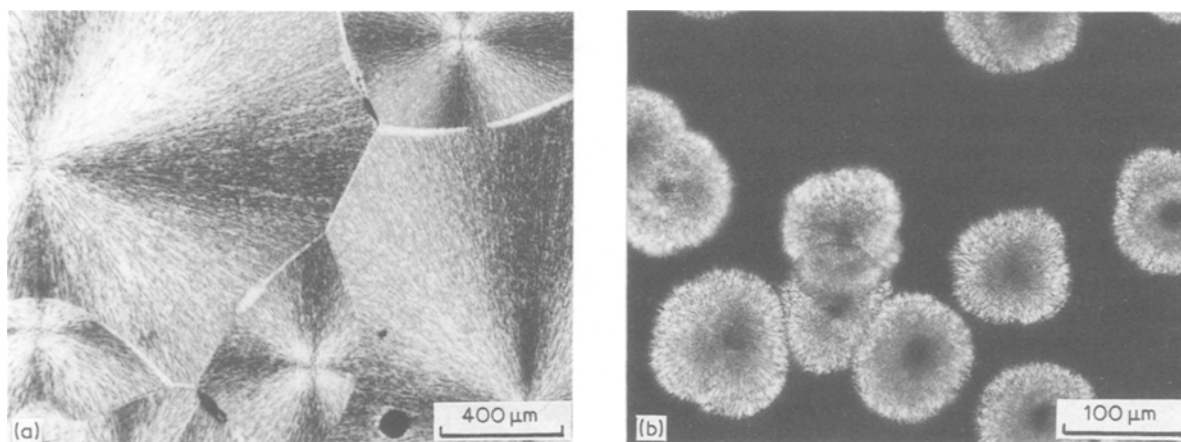


Figure 2 Transmission optical micrographs of (a) semicrystalline PEO, SPEO, grown at 30°C from a melt with $X = 0$; (b) CC grown at 65°C from a melt with $X = 0.091$. Note different magnifications.

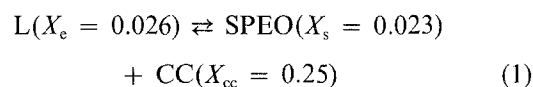
dissolved in semicrystalline PEO must reside in non-crystalline regions, the logical inference is that the solubility limit ($X_s = 0.023$ in Fig. 1) would be lower in SPEO having a smaller noncrystalline fraction. In the limit of unit crystallinity this solubility would decrease to zero; it is likely that $X_s \approx 0$ in the highly crystalline "SPEO" used by Robitaille *et al.* [9]. Despite these rather subtle distinctions regarding SPEO, the heat of fusion of CC observed in our melt-equilibrated system, $\Delta H_{cc} = 171 \text{ J g}^{-1}$, is identical to that reported by Robitaille *et al.* [9]. It appears that polymer molecular weight does not influence the composition of the complex crystalline phase. Figure 1 is thus a "pseudo-equilibrium" phase diagram, as the nature of the terminal SPEO "phase" is determined by kinetic parameters associated with the crystallization of PEO from the melt. This nonequilibrium nature of the polymer component has been recognized since the pioneering work of Smith and Pennings [15, 16] on binary eutectics of polyethylene and tetrachlorobenzene.

3.2. General morphological features

Optical microscopy provides a convenient technique for observing the solidification process. The two terminal phases in the partial phase diagram, SPEO and CC, have quite distinct appearances. SPEO grows as large spherulites (Fig. 2a), characterized in polarized transmission by the "Maltese cross" indicative of a particle with different polarizabilities in the radial and tangential directions. The CC phase appears quite

different; Fig. 2b is of complex crystalline particles grown under equilibrium conditions in the two phase field ($X = 0.091$, $T_c = 65^\circ \text{C}$, $t_c = 22 \text{ h}$). Polycrystalline CC is birefringent, but not spherulitic. Lee and Wright [17] studied the morphology of PEO–NaSCN, $X = 0.20$, by transmission electron microscopy. The melt crystallized mixture (mostly CC) showed no evidence of spherulites. Robitaille *et al.* [9], on the other hand, have grown conspicuously spherulitic CC from the melt at $T_c = 100^\circ \text{C}$. The reasons for this discrepancy are not understood.

Nonequilibrium solidification from the melt is the rule, not the exception in these systems. For $X < X_e$, solidification results in conventional spherulitic SPEO which is virtually identical to salt-free polyethylene oxide; growth rates and undercoolings likewise are not substantially modified by the presence of moderate amounts of salt in the liquid phase. The same situation obtains for eutectic liquid (L), since the product of the eutectic reaction



is 99 mol % (98 wt %) SPEO, and the presence of $\sim 1\%$ CC is difficult to detect. The nonequilibrium solidification of a hypereutectic liquid ($X = 0.067$) is illustrated in Fig. 3. Spherulites grow first, apparently filling the volume of the system (Fig. 3a and b). That these are SPEO (as opposed to CC) can be deduced

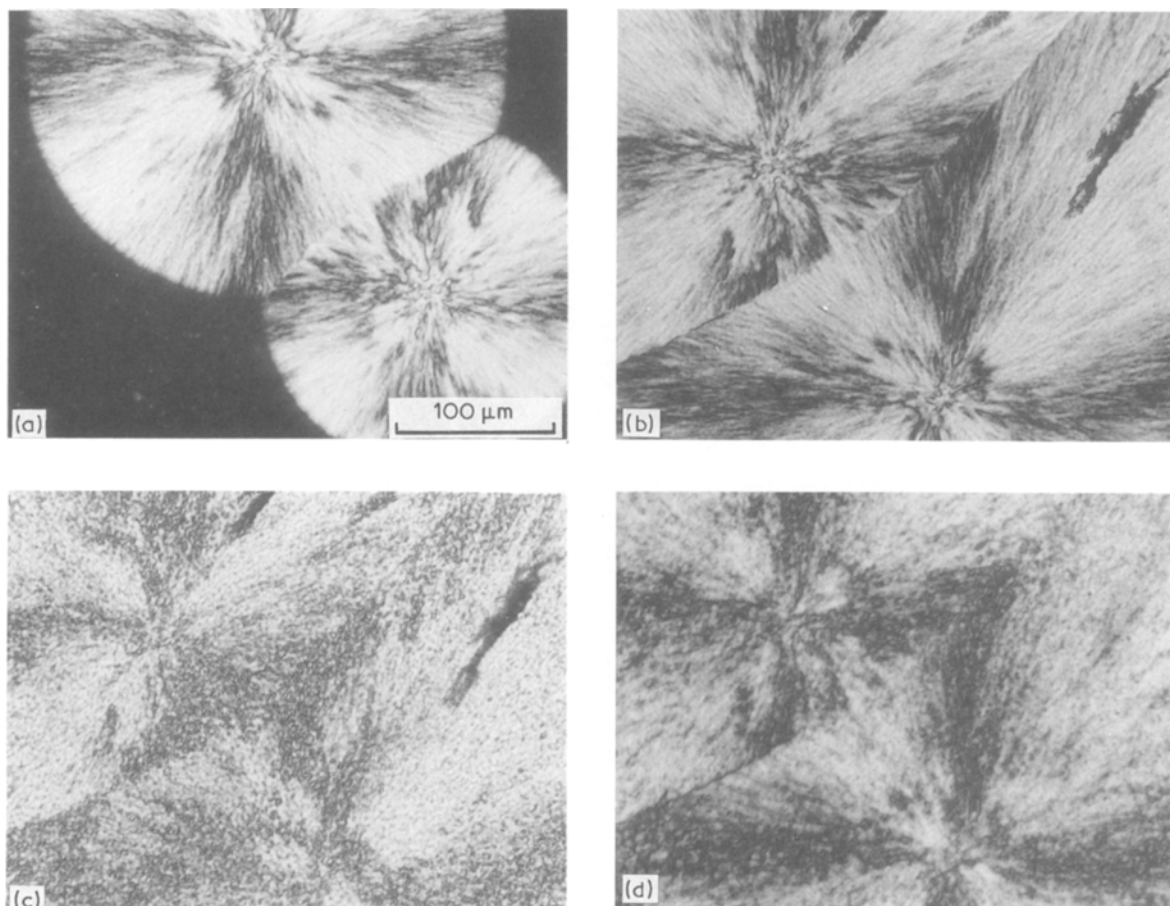


Figure 3 Isothermal crystallization of PEO–NaSCN, $X = 0.067$, $T_c = 30^\circ \text{C}$. (a) $t_c = 1 \text{ min}$, primary SPEO; (b) $t_c = 3 \text{ min}$, primary SPEO; (c) $t_c = 100 \text{ min}$, primary plus coupled growth; (d) $t_c = 100 \text{ min}$, heated to 100°C , CC microcrystals.

from general appearance and from the fact that, if heated at this stage, they melt completely below 65°C. At much longer times a second crystallization process is indicated by the mottled appearance acquired by the primary spherulites (Fig. 3c). This is attributed to a coupled growth or eutectic reaction in liquid pools of undetermined size trapped within the SPEO spherulites. The volume change on crystallization of these regions causes strains which disrupt the optical symmetry of the spherulites. That CC has been formed at this stage can be seen by heating (Fig. 3d). SPEO, formed as primary spherulites or in the subsequent coupled growth reaction, melts at $T_c = 63^\circ\text{C}$. Above this temperature CC persists as very small birefringent crystallites. These were observed to melt below 120°C, less than the liquidus temperature of 125°C (Fig. 1). It is reasonable that CC grown rapidly under these non-equilibrium conditions would have defects which lower the melting temperature. Note that the optical characteristics of the melted spherulite are retained above T_c , in fact enhanced from those in Fig. 3c. The orientation of CC microcrystals formed during coupled growth is influenced by the spherulitic “skeleton” in which they are formed. This same “ghost spherulite” composed of stable complex crystals above T_c was seen by Robitaille and Fauteux [8] in PEO–LiClO₄. A similar oriented secondary crystallization of long-chain-branched polyethylene in spherulites of linear polyethylene was reported by Kyu *et al.* [18].

Quite different behaviour is observed for undercooled liquids having appreciably higher salt concentrations. Primary CC is formed at $T_c = 30^\circ\text{C}$ in the $X = 0.11$ system (Fig. 4a). This phase is not “volume filling” (compared to SPEO spherulites, Fig. 3b), and generally resembles carefully grown CC particles (Fig. 2b). At longer times coupled growth occurs in the unconverted liquid regions (Fig. 4b), leading to a mottled, irregularly birefringent pattern with a characteristic length scale of about 5 μm for the inhomogeneity. In this case one can see faint images of the primary CC particles beneath the eutectic solid. No particular optical effects are noted on heating this solidified system through T_c ; the gradual melting process is concluded at 155°C, again below the equilibrium liquidus temperature of 165°C (Fig. 1).

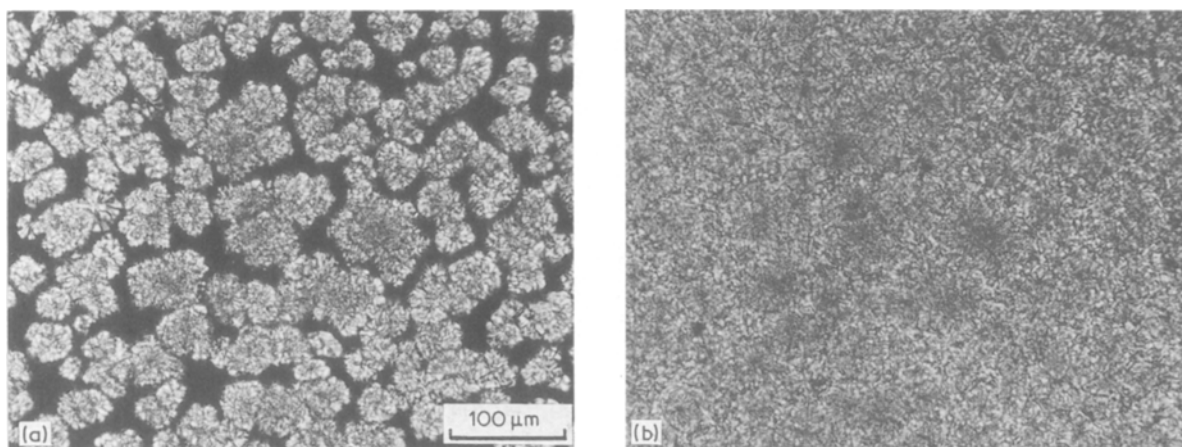


Figure 4 Isothermal crystallization of PEO–NaSCN, $X = 0.111$, $T_c = 30^\circ\text{C}$. (a) $t_c = 1$ min, primary CC; (b) $t_c = 45$ min, primary plus coupled growth.

3.3. DSC studies

DSC scans of two systems solidifying at $T_c = 23^\circ\text{C}$ are shown in Figs 5 and 6. For $X = 0.067$, the quenched mixture is amorphous, with $T_g = 236\text{K}$ (-37°C), followed by equal exotherm and endotherm corresponding to crystallization and melting of SPEO. Crystallizing for 1 min at 23°C permits the primary SPEO spherulites to grow, and the glass transition temperature of the remaining liquid is shifted upwards to $T_g = 255\text{K}$ (-18°C). Further growth at 23°C is characterized by a relatively slow increase of SPEO and CC, the latter melting over a range bordered by $T \approx 110^\circ\text{C}$. During this second crystallization process the glass temperature T_g of the unconverted liquid is constant at 255 K (the apparent C_p step above 300 K is due to annealing the original SPEO crystals at that temperature, and is not a glass transition). T_g can be converted to salt concentration in the amorphous regions by the relation

$$T_g(\text{K}) = 208 + 423 X_L \quad (2)$$

generated from this series of quenched PEO–NaSCN samples. From Equation 2 we conclude that $X_L = 0.111$ for the liquid which is solidifying. The amount of this liquid decreases during the course of coupled growth, and the heat capacity step is unobservable in the final product (Fig. 5, $t_c = 20$ min). The interlamellar amorphous regions in SPEO do not have a calorimetrically observable T_g , an effect which has been documented with semicrystalline polycarbonate [19].

For $X = 0.11$, the overall crystallization kinetics are much slower. Here CC is formed first (Fig. 6, $T_c = 40$ min) and SPEO is observed later. T_g of the liquid phase shifts downward from 255 to 248 K during crystallization at 23°C , implying a liquid with $X_L = 0.092$. Again no T_g is observed after solidification is complete.

In a study of quenched PEO–NaSCN mixtures, Rabitaille *et al.* [9] noticed T_g values in partially crystallized samples which were higher than those corresponding to bulk amorphous regions having the same (assumed) salt concentration. It is believed that this effect is due to changes in local salt concentration, and not to constraints from the CC or PEO crystallites.

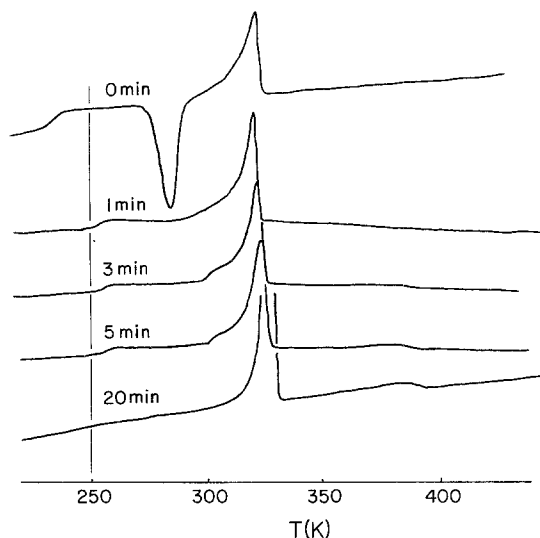


Figure 5 DSC traces of melt quenched PEO-NaSCN, $X = 0.067$, after crystallization at $T_c = 300$ K (23°C) for the indicated times. Vertical line at $T = 250$ K is for reference.

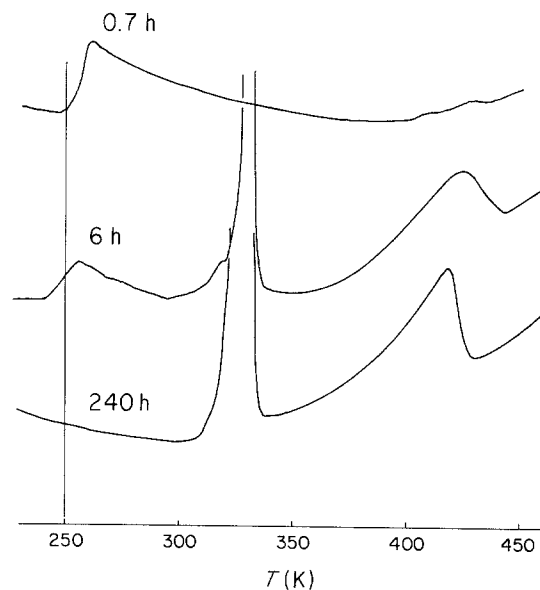


Figure 6 DSC traces of melt quenched PEO-NaSCN, $X = 0.111$, after isothermal crystallization at $T_c = 300$ K (23°C) for indicated times. Original quenched sample ($t_c = 0$) has $T_g = 255$ K.

3.4. Coupled growth

The solidification of undercooled liquids of PEO-NaSCN conforms to coupled growth or eutectic solidification [12, 13] at a composition X'_c not equal to the equilibrium eutectic liquid X_e . In this case one has a skewed zone of coupled growth, i.e. $X'_c > X_e$, caused by the relatively slow growth of CC. The location of this zone can be determined from the value of $X'_c = X_L$ obtained from the (time invariant) T_g of the liquid during the coupled growth reaction:

$$L(X'_c) \rightarrow \text{SPEO}(X_s = 0.023) + \text{CC}(X_{cc} = 0.25) \quad (3)$$

Here it is assumed that the product compositions of the nonequilibrium eutectic reactions are the same as for the equilibrium case (Equation 1). While this is difficult to prove, there is no strong evidence to the contrary. It may be that SPEO grown at larger undercoolings has a larger interlamellar amorphous fraction and hence a larger X_s , but annealing mechanisms are active at these growth temperatures (near T_m) which would serve to increase crystallinity to a fairly con-

stant value. Experiments like those in Fig. 3 show that CC formed at large undercoolings (either primary or coupled growth products) melt at lower temperatures. Though it is possible that an altered stoichiometry is involved, more likely it is an enthalpy defect occasioned by the (relatively) rapid growth at large undercoolings. In any event, the focus of this study is X'_c , which is determined directly by T_g of the solidifying liquid. Small perturbations of the solid compositions are not important in this context.

DSC was used to monitor isothermal crystallization over the range $310 \geq T_c \geq 280$ K, and the observed X'_c resulting from application of Equation 2 are summarized in Fig. 7. From replicate measurements on these partially crystallized systems, T_g is precise to ± 1 K, with X'_c thus estimated to better than ± 0.003 . Shown by a dashed line is an extension of the SPEO liquidus curve formed by simple extrapolation.

Data for three systems are presented in Fig. 7. Those for $X = 0.067$ and $X = 0.091$ are virtually

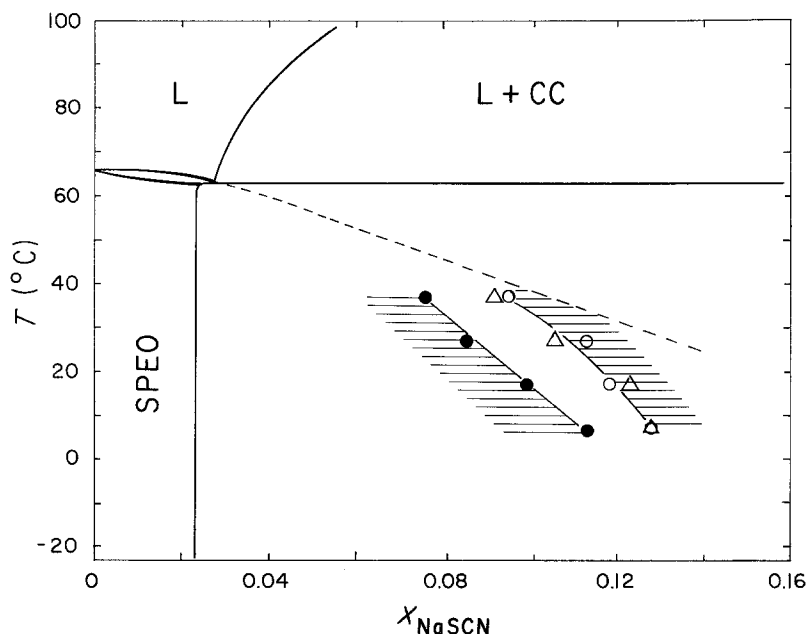


Figure 7 Location of coupled growth zones for PEO-NaSCN having $X = 0.067$ (\circ), $x = 0.091$ (Δ) and $x = 0.143$ (\bullet). Dashed line represents the metastable liquidus of the SPEO phase.

indistinguishable, while the loci of X'_c for the most concentrated system ($X = 0.143$) lie at lower values. In the two former cases, growth of primary SPEO spherulites was observed at all temperatures. Despite the fact that the undercooling of SPEO (calculated by reference to the metastable liquidus) is less than that of CC (referred to the equilibrium liquidus), SPEO growth is much faster. As primary solidification proceeds, X_L increases, increasing the undercooling of CC and decreasing that of SPEO. When the growth rates of the two phases become comparable, coupled growth occurs at $X_L = X'_c$. At lower crystallization temperatures X'_c is larger because the growth rate of the more severely undercooled CC is retarded by a larger factor. The same reasoning is applied to solidification of the $X = 0.143$ system, though here the undercooling of CC is so large that it precipitates first. This reaction reduces X_L , decreasing the undercooling and growth rate of CC and increasing the undercooling of SPEO until coupled growth occurs at X'_c .

It was anticipated that these two sets of experiments, involving the approach of X_L to X'_c from high or low concentrations, would serve to define the composition width of the coupled growth zone. The expectation was that the X'_c curve for the primary CC curve ($X = 0.143$) would lie to the right of that from the primary SPEO samples. There is, however, an "overshoot" which renders the two sets of experiments incompatible in detail; the hatched areas indicate the general locations of the coupled growth zones, the widths of which are unknown. The most logical explanation for this "overshoot" involves nucleation of the absent phase. For the low X case, an additional undercooling (larger X'_c) apparently is required to cause CC to grow at the desired rate. Conversely, in the high X case X'_c must be forced to lower values to increase the undercooling of the SPEO phase which is absent during primary growth. It may be that only one of these nucleation problems exists. It has been observed in these studies that (primary) CC can nucleate the growth of SPEO, though it is impossible to devise an experiment to check the nucleation of CC by SPEO. Assuming that the latter does constitute an additional kinetic hindrance to the start of coupled growth, the leftmost zone in Fig. 7 would be considered most "correct" in that it is not shifted by nucleation effects. Another possible cause of the different behaviours may lie in gross morphology. For the low X experiments coupled growth occurs in liquid pools within primary SPEO spherulites, and this restriction (as opposed to bulk liquid conversion in high X samples) could somehow modify the location of the eutectic zone.

4. Conclusions

Undercooled liquids of PEO–NaSCN are shown to solidify in two stages; primary growth of the fastest

growing phase is followed by coupled growth at a nonequilibrium eutectic composition X'_c determined by the crystallization temperature T_c . While Smith and Pennings [16] observed a skewed coupled growth zone in a binary polyethylene–solvent system, this present work is thought to be first demonstration of nonequilibrium eutectic solidification where both phases are polymeric. The ability to determine the composition of the eutectic liquid by DSC makes quantitative study of this system particularly tractable. While most observations are accounted for by the coupled growth model, the "overshoot" of growth zones from different composition regimes deserves further study.

Acknowledgements

This research was supported by the National Science Foundation's MRL program (DMR-85 20280) with funds administered by the Northwestern University Materials Research Center. We greatly appreciate many helpful discussions with Professor P. W. Voorhees.

References

1. M. ARMAND, *Solid State Ionics* **9 & 10** (1983) 745.
2. J. S. TONGE and D. F. SHRIVER, in "Polymers in Electronics", edited by J. Lai (CRC Press, Cleveland, Ohio, 1989) in press.
3. C. BERTHIER, W. GORECKI, M. MINIER, M. B. ARMAND, J. M. CHABAGNO and P. RIGAUD, *Solid State Ionics* **11** (1983) 91.
4. Y. L. LEE and B. CRIST, *J. Appl. Phys.* **60** (1986) 2683.
5. P. R. SORESENSEN and T. J. JACOBSEN, *Polym. Bull.* **9** (1983) 47.
6. M. STAINER, L. C. HARDY, D. H. WHITMORE and D. SHRIVER, *J. Electrochem. Soc.* **131** (1984) 784.
7. M. MINIER, C. BERTHIER and W. GORECKI, *J. Phys. (Paris)* **45** (1984) 739.
8. C. D. ROBITAILLE and FAUTEUX, *J. Electrochem. Soc.* **133** (1986) 315.
9. C. ROBITAILLE, S. MARQUES, D. BOILS and J. PRUD'HOMME, *Macromolecules* **20** (1987) 3023.
10. J. D. HOFFMAN, G. T. DAVIS and J. L. LAURITZEN Jr, in "Treatise on Solid State Chemistry", Vol. 3, edited by N. B. Hannay (Plenum Press, New York, 1976) p. 497 ff.
11. Y. L. LEE, PhD thesis, Northwestern University, 1987.
12. W. KURZ and D. J. FISHER, *Intnl. Metals Rev.* **24** (1979) 177.
13. *Idem*, in "Fundamentals of Solidification" (Trans Tech Publications, Aedermannsdorf, Switzerland, 1986) pp. 113–116.
14. C. P. BUCKLEY and A. J. KOVACS, *J. Colloid. Polym. Sci.* **254** (1976) 695.
15. P. SMITH and A. J. PENNING, *Polymer* **15** (1973) 413.
16. *Idem*, *J. Mater. Sci.* **11** (1976) 1450.
17. C. C. LEE and P. V. WRIGHT, *Polymer* **23** (1982) 681.
18. T. KYU, S. R. HU and R. S. STEIN, *J. Polym. Sci.: Part B: Polym. Phys.* **25** (1987) 89.
19. G. E. WISSLER and B. CRIST, *ibid.* **18** (1980) 1257.

Received 20 May

and accepted 13 September 1988